Proceedings of the ASME 2009 Dynamic Systems and Control Conference
DSCC2009
October 12-14, 2009, Hollywood, California, USA

DSCC2009-2708

TOLERANT ETHANOL ESTIMATION IN FLEX-FUEL VEHICLES DURING MAF SENSOR DRIFTS

Kyung-ho Ahn[*], **Anna G. Stefanopoulou**
The University of Michigan
Ann Arbor, Michigan 48109

Mrdjan Jankovic
Ford Research and Advanced Engineering
Dearborn, Michigan 48121

ABSTRACT

Flexible fuel vehicles (FFVs) can operate on a blend of ethanol and gasoline in any volumetric concentration of up to 85% ethanol (93% in Brazil). Existing FFVs rely on ethanol sensor installed in the vehicle fueling system, or on the ethanol-dependent air-to-fuel ratio (AFR) estimated via an exhaust gas oxygen (EGO) or λ sensor. The EGO-based ethanol detection is desirable from cost and maintenance perspectives but has been shown to be prone to large errors during mass air flow sensor drifts [1, 2]. Ethanol content estimation can be realized by a feedback-based fuel correction of the feedforward-based fuel calculation using an exhaust gas oxygen sensor. When the fuel correction is attributed to the difference in stoichiometric air-to-fuel ratio (AFR) between ethanol and gasoline, it can be used for ethanol estimation. When the fuel correction is attributed to a mass air flow (MAF) sensor error, it can be used for sensor drift estimation and correction. Deciding under which condition to blame (and detect) ethanol and when to switch to sensor correction burdens the calibration of FFV engine controllers. Moreover, erroneous decisions can lead to error accumulation in ethanol estimation and in MAF sensor correction. In this paper, we present a cylinder air flow estimation scheme that accounts for MAF sensor drift or bias using an intake manifold absolute pressure (MAP) sensor. The proposed fusion of the MAF, MAP and λ sensor measurements prevents severe mis-estimation of ethanol content in flex fuel vehicles.

NOMENCLATURE

AFR_s Stoichiometric air-to-fuel ratio
e Volume fraction of ethanol in ethanol-gasoline blend
e_m Mass fraction of ethanol in ethanol-gasoline blend
p_m Intake manifold absolute pressure
R Gas constant
T_m Intake manifold temperature
V_d Total displaced cylinder volume
V_m Intake manifold volume
W_{cyl} Air flow rate into the cylinder
W_{fb} Feedback fuel flow command
W_{ff} Feedforward fuel flow command
W_{ff1} Feedforward fuel flow command not compensated by the fuel puddle dynamics
W_θ Air flow rate through the throttle
α_{tr} Triggering signal for switching between ethanol adaptation and others
β_{tr} Triggering signal for switching on MAF sensor drift adaptation
η_v Volumetric efficiency
θ Throttle angle
λ Ratio of actual AFR to stoichiometric AFR, measured by an EGO sensor
τ_{MAF} MAF sensor time constant

1 INTRODUCTION

Currently available flexible fuel vehicles can operate on a blend of ethanol and gasoline in any concentration of up to 85% ethanol. This blend is denoted by the EXX nomenclature, where XX represents the volumetric percentage of ethanol in the blend. The United States commonly uses E85 as an alternative to the normal E0 or gasoline fuel. In Brazil, however, the fuel blend also contains water and E100 refers to a blend of 93% of ethanol and 7% of water [3]. Such fuel blends mixed with additional water are not considered in this paper. Flexible fuel vehicles are currently being offered by many manufacturers.

The characteristics of ethanol differ from those of gasoline, as shown in Tab. 1. Various effects of ethanol fuel on a spark ignition engine are well reported in [4]. Often ethanol fuel is associated with driveability and startability problems in cold and

[*]Address all correspondence to akyungho@umich.edu.

Table 1. PROPERTIES OF ETHANOL COMPARED WITH GASOLINE.

Property	Gasoline	Ethanol
Research Octane Number (RON)	92	111
Density (kg/m^3)	747	789
Heat of combustion (MJ/kg)	42.4	26.8
Stoichiometric air-to-fuel ratio	14.6	9.0
Boiling point (°C)	–	78.5
Latent heat of evaporation (kJ/kg)	420	845

hot weather [5,6] and at high altitude [7]. Existing FFVs achieve lower range (miles driven per tank) when operating on high ethanol content fuel due to its lower combustion heating value as compared to gasoline. However, as shown in Tab. 1 ethanol has a higher octane ratio and therefore, a higher compression ratio and higher combustion efficiency can be obtained without knocking problems. Another advantage is that, the high vaporization heat can be used for charge cooling [8], thus improving further the knock resistance and potentially fuel economy. Given the effect of fuel variation, FFVs should embed engine calibration maps in their controllers and management systems to account for this variation. To accomplish this, the first task in a flex-fuel strategy is to estimate reliably the ethanol percentage. Although, this estimation is possible with the addition of a di-electric or electrochemical sensor in the fueling system, the reliability of these sensors has not yet been proven. Apart from the cost and reliability issues associated with such sensors, on-board diagnostic (OBD) requirements would require a redundant method for assessing the ethanol percent in order to diagnose the ethanol sensor faults or degradation.

Ethanol content estimation very often depends on the air-to-fuel ratio (AFR) measurement through an exhaust gas oxygen sensor immediately after refueling is detected. A simple EGO-based ethanol content estimation law and its sensitivity on MAF measurement errors is demonstrated in [2] using a phenomenological model. The ethanol content estimation relies on the assumption that any fuel feedback correction is due to miscalculation of the feedforward fuel amount due to an error in the assumed stoichiometric value of the fuel used. For example, a lean ($\lambda > 1$) EGO sensor measurement can occur when the assumed stoichiometric ratio, AFR_s, used to calculate the injected fuel necessary to match the inducted air for stoichiometric combustion, is higher than the actual. As Tab. 1 shows, this can happen when the assumed ethanol content is lower than the actual. Obviously, if the feedforward fuel miscalculation is due to errors in the cylinder air charge estimation and not entirely due to the fuel properties, the ethanol estimation will erroneously compensate for the air charge estimation error. The air charge estimation, in turn, depends on the mass air flow through the throttle body. Hence, a MAF sensor error results in steady-state ethanol content estimation error with high sensitivity. The high sensitivity problem is also shown in [1] for errors occurring in the fuel injectors or the fuel path in general. This ethanol estimation sensitivity on fuel injector errors can be explained in the same way with the MAF sensor errors since both errors will cause errors in the feedforward fuel calculation which will be mistaken as ethanol content estimation error.

If the ethanol content or the stoichiometric AFR is known, the EGO sensor reading may be used in another adaptation against MAF sensor drift/bias and injector shifts in the same manner as used in ethanol content estimation. Adapting the feedforward fuel compensation due to errors in the inlet air sensing based on the EGO-based fuel feedback compensation is now a common practice [9] referred to an air charge adaptation. Switching between two adaptations namely, the ethanol adaptation and the air charge adaptation, is then required to avoid misclassifying ethanol content variations with sensor drifts or component aging. An appropriate switching logic using the tank refill trigger and relevant process characteristics should be devised for that purpose. However, this scheme may cause accumulation of errors because every estimation needs the other's true value to guarantee convergence to its actual value even though there are no true or reference values to reset all estimations to, once a vehicle is out from a factory or a major maintenance event, or unless it operates with known fuel. This error accumulation during regular field operation will be briefly discussed in this paper.

This paper focuses on the cylinder air flow estimation under MAF sensor drift or bias using an intake manifold absolute pressure sensor in order to prevent severe mis-estimation of ethanol content in flex fuel vehicles. The estimation scheme is independent of the exhaust gas oxygen sensor measurement. Therefore, the switching between this compensation of MAF sensor drift and the ethanol content estimation is not necessary and the associated error accumulation problem can be avoided. Simulation is performed to demonstrate the air flow estimation with compensation of MAF sensor drift using MAP sensor and the ethanol content estimation in flex fuel vehicles.

2 ETHANOL CONTENT ESTIMATION

This section provides review on the EGO-based ethanol content estimation and the high sensitivity problem posed in [2] and briefly discusses the error accumulation problem in the switching adaptation scheme commonly using the EGO-based approach.

Figure 1 shows the block diagram of AFR control with flex fuel. The ethanol content estimation is realized through a fuel adaptation loop by integrating the fuel feedback control signal, W_{fb}:

$$\dot{\widehat{AFR}}_s = -\gamma_e W_{fb} \alpha_{tr}, \tag{1}$$

where $\widehat{AFR}_s$ denotes the estimated stoichiometric AFR of the injected fuel, γ_e is the adaptation gain, α_{tr} is a triggering variable which enables the ethanol estimation by setting it to $\alpha_{tr} = 1$ after detecting a tank refill event. The estimated AFR_s is easily converted to an estimated volumetric ethanol content, $\widehat{e}$:

$$\widehat{e}_m = \frac{14.6 - \widehat{AFR}_s}{5.6}, \quad \widehat{e} = \frac{\widehat{e}_m}{1.056 - 0.056 \times \widehat{e}_m}.$$

The fuel feedback controller can be emulated by any integral-based controller, and without loss of generality, we assume a

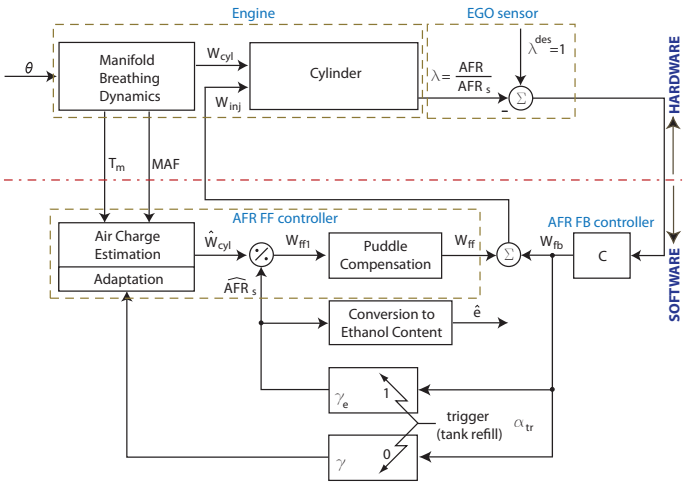

Figure 1. BLOCK DIAGRAM OF AFR CONTROL.

simple proportional-integral (PI) feedback control signal:

$$W_{fb} = C(s)(\lambda^{des} - \lambda) = -k_{PI}\frac{\tau_{PI}s+1}{s}(1-\lambda). \tag{2}$$

Suppose that a faulty MAF sensor is used and assume there is neither injector fault nor EGO sensor error. Let f_e be the MAF sensor error fraction such that $\overline{W}_\theta = (1+f_e)W_\theta$, where $\overline{W}_\theta$ is the measured mass air flow through the throttle and W_θ is the actual. The estimated steady-state ethanol content is then [2]:

$$\widehat{e}_m = e_m - f_e(2.6 - e_m). \tag{3}$$

The high sensitivity problem in ethanol content estimation under MAF sensor error in steady state is obvious in the following sensitivity expression:

$$\frac{\partial \widehat{e}_m}{\partial f_e} = -(2.6 - e_m). \tag{4}$$

The MAF sensor error fraction is amplified to ethanol content error by factor of about 2.6 for E0 and of about 1.8 for E85, respectively.

The triggering variable α_{tr} may be used to deactivate the ethanol adaptation ($\alpha_{tr} = 0$) and activate the other adaptation loop that corrects the engine maps and/or drifts in sensors and actuators. Since the ethanol content estimation is adjusted in response to any mismatch between the stoichiometric and the measured ones, the ethanol estimation could respond to the AFR errors during fast throttle modulation, i.e., transient driving conditions. To filter out these effects, a small adaptation gain γ_e in Eq. (1) is typically employed. The small adaptation gain slows down the ethanol estimation convergence rate. Even if the ethanol adaptation gain is kept high[1], there is no way to determine if the estimated ethanol content has converged to the actual value under consecutive throttle modulations. Once an erroneous estimated ethanol content is used in the MAF sensor drift correction, the error will propagate causing an erroneous cylinder air flow estimation. The cylinder air flow estimation error may again cause ethanol content estimation error when fuel adaptation is activated. In this way, errors would accumulate. Such errors are only bounded by known bound of sensor drift and physical bound of fuel ethanol content, i.e. 0-85%. The accumulation of errors cannot be observed in steady state fundamentally because the feedforward signal is determined by the coupled expression of the estimated cylinder air flow, $\widehat{W}_{cyl}$, and the estimated stoichiometric AFR, $\widehat{AFR}_s$, by $W_{ff} = \widehat{W}_{cyl}/\widehat{AFR}_s$, which is fixed in steady state. Since one estimation requires knowledge of the other's true value, a reference value to reset an estimation should be provided. However, once vehicle is manufactured or released from a major maintenance event, or unless it operates with known fuel, there is no way to reset to the true ethanol value.

Simultaneous adaptation based on the transient characteristics of system dynamics is not promising, either. Indeed, refueling is not a frequent event and an arbitrary driving scenario cannot guarantee enough variability for adapting simultaneously two unknown parameters.

In order to avoid error accumulation problem in the switching adaptation, the cylinder air flow should be estimated and account for the MAF sensor drift, independently of λ measurement. For this purpose, an intake manifold pressure sensor may be utilized. Using a manifold absolute pressure (MAP) sensor may be suitable in the sense that the associated cost is low. A conventional method from which the cylinder air flow can be calculated using MAP is the *speed-density* method:

$$W_{cyl} = \eta_v \frac{n_e}{2} V_d \frac{p_m}{RT_m}, \tag{5}$$

where p_m denotes the manifold absolute pressure, η_v is the volumetric efficiency, n_e is the engine speed (in rps) and V_d is the total displaced cylinder volume. Since η_v bears relatively high uncertainty, estimating cylinder air flow only using the MAP measurement via this equation is not a good idea. Therefore, we will still use the MAF sensor measurement and the drift will be compensated by the MAP measurement via the speed density equation. Note that any error fraction in MAP results in the same amount of error fraction in cylinder air flow from the speed-density equation:

$$\frac{\delta W_{cyl}}{W_{cyl}} = \frac{\delta p_m}{p_m}. \tag{6}$$

Therefore, the potential ethanol estimation error during MAP drift is not worse than than the ethanol estimation error during MAF drift. Moreover, MAP sensor accuracy is usually much better than MAF sensor accuracy [11, 12]. This fact justifies the idea of using MAP sensor to correct MAF sensor drift.

3 HIGH GAIN OBSERVER FOR INPUT ESTIMATION

The purpose of this section is to review the input estimation algorithm that will be used in subsequent sections for correcting MAF sensor drifts. Stotsky and Kolmanovsky have applied

[1] However, such transient responses can be much reduced by using a transient fuel compensator based on a proper flex fuel puddle model [10], enabling fast adaptation.

the following high gain observer technique to cylinder air charge estimation using a manifold pressure sensor [13]. Their work serves as a basis for the compensation of MAF sensor drift in this paper.

We consider an input estimation problem arising from a first-order dynamic system:

$$\dot{z} = y + x, \tag{7}$$

where the signals z and y are measured, but x is a unknown time-varying input which has to be estimated on line. A high gain observer is defined in terms of auxiliary variables ε and v such that the estimation of x is given by

$$\hat{x} = \gamma z - v, \tag{8}$$

where

$$\varepsilon \triangleq \hat{x} - x = \gamma z - v - x \tag{9}$$

and v satisfies

$$\dot{v} = -\gamma v + \gamma y + \gamma^2 z. \tag{10}$$

Here γ is a positive observer gain. Evaluating the derivative of v along the solutions of system equation (9) one obtains

$$\dot{\varepsilon} = -\gamma\varepsilon - \dot{x}. \tag{11}$$

Assume now that $\dot{x}$ is bounded, i.e., that there exists a positive constant b_1 such that $\sup_t \|\dot{x}(t)\| \leq b_1$. Multiplying Eq. (11) by 2ε, and using an estimate $\|2\dot{x}\varepsilon\| \leq \dot{x}^2/\gamma + \gamma\varepsilon^2$ it follows that $d\varepsilon^2/dt \leq -\gamma\varepsilon^2 + b_1^2/\gamma$ and the following transient bound for the estimation error is obtained,

$$\|\varepsilon(t)\| \leq \sqrt{\varepsilon(0)^2 e^{-\gamma t} + \frac{b_1^2}{\gamma^2}}. \tag{12}$$

Transient bound Eq. (12) implies that the upper bound on the estimation error for any $t > 0$ can be made arbitrarily small by increasing the design parameter $\gamma > 0$. Note that if one defines $\hat{z} = v/\gamma$, then Eq. (10) reduces to $\dot{\hat{z}} = -\gamma(\hat{z} - z) + y$. Thus $\hat{z}$ can be viewed as an estimate of z, provided $\gamma > 0$ is sufficiently large.

The same result can be obtained by filtering both sides of Eq. (7) with a low pass filter [13].

4 ESTIMATION OF FLOW THROUGH THE THROTTLE

4.1 MAF Sensor Dynamics Including Drift

The MAF sensor dynamics can be described by a first order lag [14]:

$$\dot{\overline{W}}_\theta = -\frac{1}{\tau_{MAF}}(\overline{W}_\theta - W_\theta), \tag{13}$$

where τ_{MAF} is the MAF sensor time constant, W_θ is the actual flow through the throttle, and $\overline{W}_\theta$ is the measured flow through the throttle by the MAF sensor.

The MAF sensor dynamics with drift can be modeled through a biased sensor gain:

$$\dot{W}_{\theta,n} = -\frac{1}{\tau_{MAF}}(W_{\theta,n} - W_\theta), \tag{14}$$

$$\overline{W}_\theta = (1 + C)W_{\theta,n}, \tag{15}$$

where $W_{\theta,n}$ is the mass air flow through the throttle body of the nominal system and C is a parameter that affects the MAF sensor gain.

The MAF sensor dynamics is then expressed as:

$$\dot{\overline{W}}_\theta = -\frac{1}{\tau_{MAF}}\left(\overline{W}_\theta - (1 + C)W_\theta\right). \tag{16}$$

4.2 Throttle Flow Estimation

To estimate the input, W_θ, the high gain observer previously discussed is utilized. Equation (16) is exactly Eq. (7) with $z = \overline{W}_\theta$, $y = -(1/\tau_{MAF})\overline{W}_\theta$ and $x = (1/\tau_{MAF})(1 + C)W_\theta$. Thus, we apply the input observer, Eq. (10) and Eq. (8), to Eq. (16):

$$\dot{v}_f = -\gamma_f v_f - \frac{\gamma_f}{\tau_{MAF}}\overline{W}_\theta + \gamma_f^2 \overline{W}_\theta, \tag{17}$$

$$\widehat{W}_C = \tau_{MAF}(\gamma_f \overline{W}_\theta - v_f), \tag{18}$$

where W_C is defined as

$$W_C \triangleq (1 + C)W_\theta, \tag{19}$$

$\widehat{W}_C$ is the estimation of W_C and γ_f is an observer gain. If we know the sensor drift C, from the adaptation in section 6, we can estimate W_θ:

$$\widehat{W}_\theta = \widehat{W}_C/(1 + C), \tag{20}$$

where $\widehat{W}_\theta$ is the estimation of W_θ.

5 ESTIMATION OF ENGINE CYLINDER FLOW

This section restates the same observer design as discussed in [13], which utilizes an intake manifold absolute pressure (MAP) sensor to estimate the engine cylinder flow. The same observer can be effectively utilized to compensate for the volumetric efficiency variation caused by ethanol content variation in gasoline-ethanol blended fuel.

5.1 Manifold Filling Dynamics

The intake manifold filling dynamics is modeled as an isothermal intake manifold pressure model:

$$\dot{p}_m = \frac{RT_m}{V_m}(W_\theta - W_{cyl}). \tag{21}$$

A conventional technique for estimating the cylinder flow into an spark ignition (SI) engine involves a *speed-density* equation (5). The volumetric efficiency bears uncertainty and it may be calibrated by the engine dynamometer test. In any case, the cylinder air flow can be viewed as a sum of nominal cylinder flow and an uncertainty term:

$$W_{cyl} = W_{cyl,n} + \Delta W_{cyl}, \tag{22}$$

with the nominal cylinder flow $W_{cyl,n}$ expressed as a function of MAP, p_m, engine speed, n_e, and possibly ethanol content in the fuel blend, e:

$$W_{cyl,n} = \mathcal{W}_{cyl,n}(p_m, n_e, e). \tag{23}$$

The intake manifold filling dynamics, (21), then becomes:

$$\dot{p}_m = \frac{RT_m}{V_m}(W_\theta - W_{cyl,n}) - \frac{RT_m}{V_m}\Delta W_{cyl}. \tag{24}$$

5.2 Cylinder Flow Estimation

Equation (24) is exactly the same as Eq. (7) with $z = p_m$, $y = \frac{RT_m}{V_m}(W_\theta - W_{cyl,n})$, $x = -\frac{RT_m}{V_m}\Delta W_{cyl}$. By applying the high gain observer, Eq. (10) and Eq. (8), to Eq. (24), the following input observer is obtained:

$$\dot{v} = -\gamma v + \gamma\frac{RT_m}{V_m}(W_\theta - W_{cyl,n}) + \gamma^2 p_m, \tag{25}$$

$$\widehat{\Delta W}_{cyl} = \frac{V_m}{RT_m}(v - \gamma p_m), \tag{26}$$

where $\widehat{\Delta W}_{cyl}$ is the estimation of ΔW_{cyl} and γ is an observer gain. The cylinder flow estimation is then expressed as:

$$\widehat{W}_{cyl} = W_{cyl,n} + (v - \gamma p_m)\frac{V_m}{RT_m}, \tag{27}$$

$$\dot{v} = -\gamma\frac{RT_m}{V_m}(\widehat{W}_{cyl} - W_\theta). \tag{28}$$

The intake manifold absolute pressure sensor is fast but may give noisy signals. A low pass filter can be utilized to filter out such noise. The isothermal intake manifold pressure model, Eq. (21), is used to avoid an excessive phase lag. Based on Eq. (21), a low pass filter can then be developed if W_θ and W_{cyl} are known:

$$\dot{\hat{p}}_m = \frac{RT_m}{V_m}(W_\theta - W_{cyl}) + \gamma_p(\bar{p}_m - \hat{p}_m), \tag{29}$$

where $\hat{p}_m$ is the estimated intake manifold absolute pressure and $\bar{p}_m$ is the measured pressure by the intake manifold absolute pressure sensor. Observers Eq. (28), Eq. (27) and Eq. (29) are combined to yield one observer scheme. In Eq. (28) and Eq. (27), the manifold absolute pressure, p_m, is replaced by the filtered manifold absolute pressure, $\hat{p}_m$. In Eq. (29), the cylinder flow, W_{cyl}, is replaced by the estimated cylinder flow, $\widehat{W}_{cyl}$. The combined observer is then summarized as:

$$\dot{v} = -\gamma\frac{RT_m}{V_m}(\widehat{W}_{cyl} - W_\theta). \tag{30}$$

$$\widehat{W}_{cyl} = \mathcal{W}_{cyl,n}(\hat{p}_m, n_e, e) + (v - \gamma\hat{p}_m)\frac{V_m}{RT_m}, \tag{31}$$

$$\dot{\hat{p}}_m = \frac{RT_m}{V_m}(W_\theta - \widehat{W}_{cyl}) + \gamma_p(\bar{p}_m - \hat{p}_m). \tag{32}$$

6 MAF SENSOR DRIFT ADAPTATION

The drift parameter C needs to be known to obtain the estimation of the throttle flow, $\widehat{W}_\theta$, in Eq. (20). If we can estimate the cylinder flow, W_{cyl}, independently of the MAF measurement, the throttle flow, W_θ, can be estimated using Eq. (21) with MAP measurement. Equation (21) is exactly the same as Eq. (7) with $z = p_m$, $y = -\frac{RT_m}{V_m}W_{cyl}$ and $x = \frac{RT_m}{V_m}W_\theta$. Thus, we may apply the input observer, Eq. (10) and Eq. (8), to Eq. (21).The nominal cylinder flow equation, (23), may approximate the original speed-density equation (5) very well in a limited region of operating conditions. We then use the nominal cylinder flow in applying the input observer:

$$\dot{v}_n = -\gamma_n v_n - \gamma_n\frac{RT_m}{V_m}W_{cyl,n} + \gamma_n^2 p_m, \tag{33}$$

$$\widehat{W}_{\theta,\mathcal{W}} = \frac{V_m}{RT_m}(\gamma_n p_m - v_n). \tag{34}$$

Introducing a triggering variable, β_{tr}, the following drift parameter adaptation can be utilized:

$$\dot{\widehat{C}} = \gamma_C(\widehat{W}_C - (1+\widehat{C})\widehat{W}_{\theta,\mathcal{W}})\beta_{tr}, \tag{35}$$

where β_{tr} is 1 in a limited region of operating conditions where the nominal cylinder flow equation is very good to approximate the original speed-density equation and is 0 elsewhere.

7 COMBINED SCHEME

The observers discussed so far are combined to yield one observer scheme for cylinder air flow estimation. The throttle flow observer, Eq. (17), Eq. (18) and Eq. (20), the cylinder flow and manifold absolute pressure observer, Eq. (30), Eq. (31), Eq. (32) and the MAF sensor drift parameter observer, Eq. (33), Eq. (34) and Eq. (35), are combined replacing actual variables by estimated variables:

$$\dot{v}_f = -\gamma_f v_f - \frac{\gamma_f}{\tau_{MAF}}\overline{W}_\theta + \gamma_f^2\overline{W}_\theta, \tag{36}$$

$$\widehat{W}_C = \tau_{MAF}(\gamma_f\overline{W}_\theta - v_f), \tag{37}$$

$$\widehat{W}_\theta = \widehat{W}_C/(1+\widehat{C}),, \tag{38}$$

$$\dot{v} = -\gamma\frac{RT_m}{V_m}(\widehat{W}_{cyl} - \widehat{W}_\theta), \tag{39}$$

$$\widehat{W}_{cyl} = \widehat{W}_{cyl,n} + (v - \gamma\hat{p}_m)\frac{V_m}{RT_m}, \tag{40}$$

$$\dot{\hat{p}}_m = \frac{RT_m}{V_m}(\widehat{W}_\theta - \widehat{W}_{cyl}) + \gamma_p(\bar{p}_m - \hat{p}_m), \tag{41}$$

$$\widehat{W}_{cyl,n} = \mathcal{W}_{cyl,n}(\hat{p}_m, n_e, e),, \tag{42}$$

$$\dot{v}_n = -\gamma_n v_n - \gamma_n\frac{RT_m}{V_m}\widehat{W}_{cyl,n} + \gamma_n^2\hat{p}_m, \tag{43}$$

$$\widehat{W}_{\theta,\mathcal{W}} = \frac{V_m}{RT_m}(\gamma_n\hat{p}_m - v_n), \tag{44}$$

$$\dot{\widehat{C}} = \gamma_C(\widehat{W}_C - (1+\widehat{C})\widehat{W}_{\theta,\mathcal{W}})\beta_{tr}. \tag{45}$$

8 STEADY STATE ANALYSIS

The proposed 5th order observer uses MAP, MAF, n_e and an estimated ethanol content to derive a feedforward fuel calculated, $W_{ff1} = \widehat{W}_{cyl}/\widehat{AFR}_s$, that accounts for the MAF sensor drift. The estimated ethanol is still based on Eq.(1). We omit the stability analysis although this can be achieved using a Lyapunov-like function as in [13] or evaluating closed-loop observer eigenvalues of the linearized system for selection of the 5 available gains. In this section, we evaluate the proposed scheme and the errors it can introduce. Its potential drawbacks are highlighted in order to critically evaluate its potential contributions. For steady-state analysis, we assume that there is no noise in MAP measurement,

i.e. $\bar{p}_m = p_m$. The calculation is straightforward by setting all state equations or all state derivatives to zero. In equilibrium computation, the state equation (45) is automatically set to zero if $\beta_{tr} = 0$. From all state equations other than Eq. (45), the steady-state results are obtained:

$$W_\theta = W_{cyl}, \tag{46}$$

$$\overline{W}_\theta = \widehat{W}_C = (1+C)W_\theta = (1+C)W_{cyl}, \tag{47}$$

$$\hat{p}_m = p_m, \tag{48}$$

$$\widehat{W}_{cyl} = \widehat{W}_\theta = \widehat{W}_C/(1+\widehat{C}) = \overline{W}_\theta/(1+\widehat{C}) = \frac{1+C}{1+\widehat{C}}W_\theta = \frac{1+C}{1+\widehat{C}}W_{cyl}, \tag{49}$$

$$\widehat{W}_{\theta,\mathcal{W}} = \widehat{W}_{cyl,n} = W_{cyl,n}. \tag{50}$$

The steady-state estimation errors are then:

$$\widetilde{W}_{cyl} = \widetilde{W}_\theta = \frac{\widehat{C}-C}{1+\widehat{C}}W_{cyl} = -\frac{\widetilde{C}}{1+\widehat{C}}W_{cyl}, \tag{51}$$

$$\tilde{p}_m = 0, \tag{52}$$

where estimation errors are defined as: $\widetilde{W}_{cyl} \triangleq W_{cyl} - \widehat{W}_{cyl}$, $\widetilde{W}_\theta \triangleq W_\theta - \widehat{W}_\theta$, $\widetilde{C} \triangleq C - \widehat{C}$ and $\tilde{p}_m \triangleq p_m - \hat{p}_m$. From Eq. (51), we can consider three different special cases.

1. If there is no steady-state error in drift parameter estimation ($\widetilde{C} = 0$), there is no error in cylinder air flow estimation in steady state:
$$\widetilde{W}_{cyl}\big|_{\widetilde{C}=0} = 0. \tag{53}$$
This is a desirable result because our estimation purpose is to enhance accuracy of cylinder air flow estimation by correcting MAF sensor drift.
2. Even if there is no MAF sensor drift ($C = 0$), the proposed cylinder estimation will rely on the estimated sensor drift with following cylinder air flow estimation error in steady state:
$$\widetilde{W}_{cyl}\big|_{C=0} = \frac{\widehat{C}}{1+\widehat{C}}W_{cyl}. \tag{54}$$
In this case, if MAF sensor drift compensation fails to estimate the actual value ($C = 0$) correctly, it may cause undesirable cylinder air flow estimation error which would not appear were it not for the drift compensation. Since the drift parameter estimation depends on the accuracy of the nominal cylinder flow expression, Eq. (23), and is not always activated according to the switching trigger β_{tr}, mis-estimation of the drift parameter is not negligible indeed.
3. If there is no MAF sensor drift compensation ($\widehat{C} = 0$), there is the following cylinder air flow estimation error in steady state:
$$\widetilde{W}_{cyl}\big|_{\widehat{C}=0} = -CW_{cyl}. \tag{55}$$
This case corresponds to use of a conventional cylinder flow estimation scheme without any compensation of MAF sensor drift. The estimation error of Eq. (55) results in amplified error in ethanol content estimation after all, hence motivating our drift compensation scheme discussed so far.

Equation (54) shows estimation performance degradation unnecessarily caused by using the estimation algorithm proposed in this paper if there is actually no MAF sensor drift at all. However, Eq. (55) shows why the proposed algorithm is worth using if the MAF sensor drift is not actually negligible.

In a region of operating conditions where the nominal cylinder flow equation is a very good approximation of actual cylinder air flow, i.e. $\beta_{tr} = 1$, the following equilibrium equation holds from Eq. (45):

$$\widehat{W}_C = (1+\widehat{C})\widehat{W}_{\theta,\mathcal{W}}. \tag{56}$$

The following steady-state estimation results are then immediately obtained from Eq. (49) and Eq. (50):

$$\widehat{W}_{cyl} = \widehat{W}_\theta = W_{cyl,n}, \quad \widehat{C} = C + (1+C)\frac{\Delta W_{cyl}}{W_{cyl,n}}. \tag{57}$$

Steady-state estimation errors are then:

$$\widetilde{W}_{cyl} = \widetilde{W}_\theta = \Delta W_{cyl}, \quad \widetilde{C} = -(1+C)\frac{\Delta W_{cyl}}{W_{cyl,n}}. \tag{58}$$

If a cylinder flow equation perfectly fits to the actual cylinder air flow, i.e. $\Delta W_{cyl} = 0$, there will be no errors in cylinder air flow estimation and drift parameter estimation as shown in Eq. (58), i.e. $\widetilde{W}_{cyl} = 0$ and $\widetilde{C} = 0$.

9 SIMULATION

Simulation of cylinder air flow estimation under MAF sensor drift is performed in the configuration of AFR control with ethanol content estimation as shown in Fig. 1. Note that a measured intake pressure signal is additionally provided to the air charge estimation block in Fig. 1 in this simulation. We use the same manifold breathing dynamics as provided in [15] and the cylinder block is simulated with a fuel puddle model developed for a port fuel injected (PFI) flex-fuel engine [16]. The puddle compensation block is realized by a transient fuel compensator using the fuel puddle model in [16]. In Eq.(15), the drift parameter C may actually vary very slowly around zero:

$$\overline{W}_\theta = (1+C(t))W_{\theta,n},$$

In this simulation, the following first order drift model is utilized to give slow variation of drift parameter, $C(t)$:

$$\dot{W}_z = -\frac{1}{\tau_z}(W_z - W_\theta), \quad C = \bar{C}W_z,$$

where the drift time constant $\tau_z = 60\,\text{sec}$ and the drift gain $\bar{C} = 5.0\,\text{sec/kg}$ are used. Figure 2 shows the cylinder air flow versus manifold absolute pressure, p_m, at a fixed engine rpm used in the simulation. The solid line is for the actual flow, W_{cyl}, and is used in the engine simulation, and the dashed line is the nominal flow, $W_{cyl,n}$, modeled by the nominal speed-density equation and used in the observer. This deviation emulates possible uncertainty in speed-density equation. Note that the nominal cylinder flow is close to the actual around $p_m = 0.5\,\text{bar}$. Therefore, we assume that the known region of operation conditions for good speed-density approximation is around $p_m = 0.5\,\text{bar}$ for simulation. Parameters and observer gains used in simulation are sum-

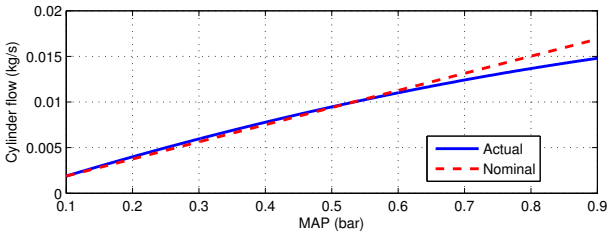

Figure 2. CYLINDER AIR FLOW AT 2000 RPM.

Table 2. PARAMETERS AND OBSERVER GAINS USED IN SIMULATION.

Parameters	Value	Unit	Gains	Values	Unit
τ_{MAF}	0.02	sec	γ_f	27	$\sec^{-1}$
$\frac{RT_m}{V_m}$	413.28	bar/kg	γ	9	
			γ_p	17	
$\eta_{v,n}\frac{V_d}{V_m}$	0.46554	cycle^{-1}	γ_n	5	
			γ_c	4	

marized in Tab. 2. These gains were tuned by looking at eigenvalues of the linearized closed-loop observer system matrix.

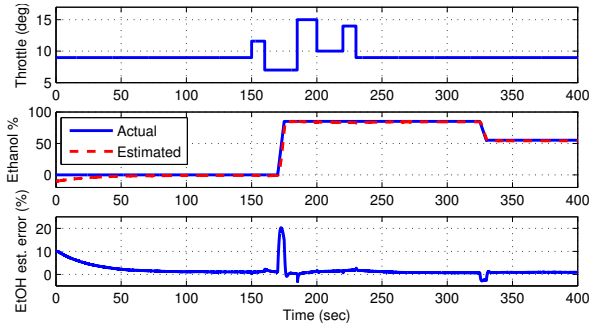

Figure 3. SIMULATED INPUTS.

Figure 3 shows simulated inputs, the throttle angle and the ethanol content. Throttle is modulated with a sequence of several step changes emulating tip-ins and tip-outs. The ethanol content is changed from zero, which means gasoline, to 85 % with a ramp profile and then it is changed to 55 % later again with a ramp profile. The second plot also depicts the estimated ethanol content which is very sensitive to cylinder air flow estimation error. The third plot shows the ethanol content estimation error. We can observe that the steady-state error is quite allowable actually due to the improved estimation of cylinder air flow. The ethanol content estimation error reduces as time goes by in the first several seconds and this is due to the fact that the estimated drift parameter, $\widehat{C}$, converges closer to the actual as shown in Fig. 5. Figure 4 shows estimation results. MAP measurement is corrupted adding white noise to the simulated actual manifold absolute pressure. We can observe reduced noise level in the filtered pressure signal without much lag in Fig. 4(a). Performance of the throttle air flow estimation and the cylinder flow estimation is quite good. Nominally estimated signals, $\widehat{W}_{\theta,\mathcal{W}}$ and $\widehat{W}_{cyl,n}$, show big errors in operating conditions where the nominal speed-density equation

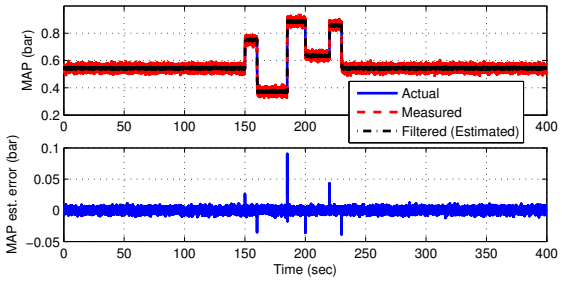

(a) MAP

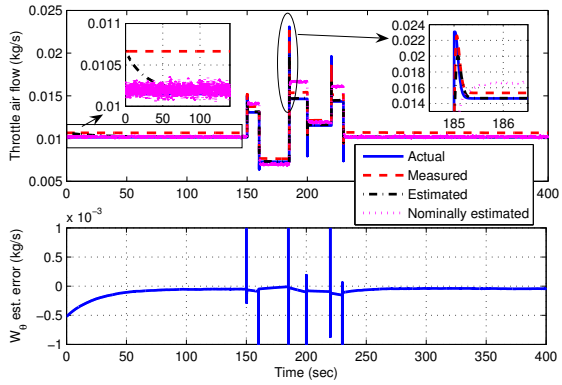

(b) throttle flow

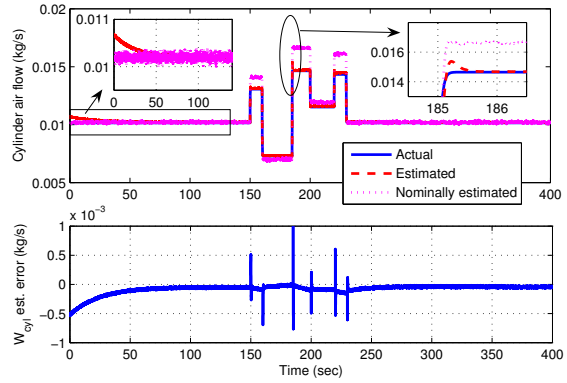

(c) cylinder air flow

Figure 4. ESTIMATION RESULT.

suffers from large deviation from the actual. Figure 5 shows the drift parameter estimation and the trigger which changes according to operating conditions. Note that steady-state error in drift parameter estimation remains even if β_{tr} is set to 1 because the (nominal) modeled cylinder flow through the speed density equation differs from the actual cylinder air flow equation. The triggering for this simulation is designed at 2000 engine rpm as:

$$\bar{\beta}_{tr}(t) = \begin{cases} 1 & \text{if } 0.4\,\text{bar} \le \hat{p}_m < 0.6\,\text{bar} \\ 0 & \text{otherwise} \end{cases}, \tag{59}$$

$$\beta_{tr}(t) = \bar{\beta}_{tr}(t) \times \bar{\beta}_{tr}(t - 0.5) \tag{60}$$

to avoid chattering. Figure 6(a) shows the λ output and Fig. 6(b)

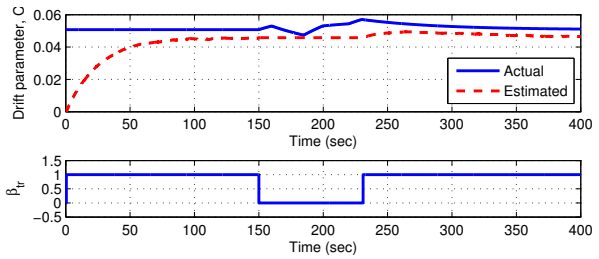

Figure 5. DRIFT ESTIMATION.

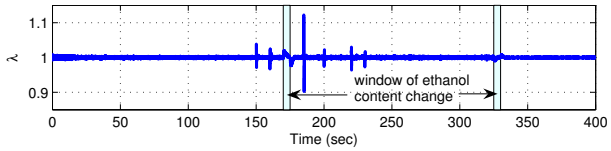

(a) simulated λ

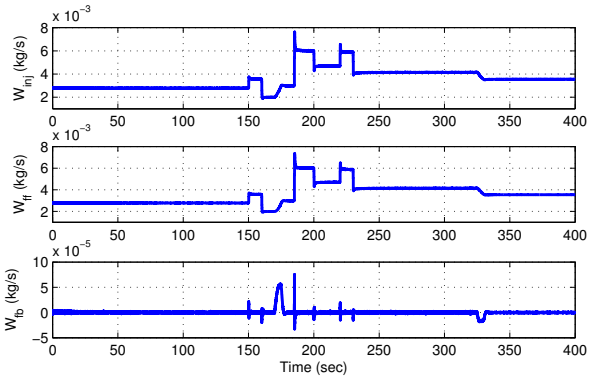

(b) simulated fuel injection

Figure 6. SIMULATED λ and FUEL INJECTION.

shows the controlled fuel injection results. The air-to-fuel ratio is regulated around stoichiometry. And the PI feedback signal enables the ethanol content estimation. We can observe that the total fuel injection and feedforward fuel injection increase in the interval of ethanol content change. Again, the ethanol content estimation is always possible as long as the feedback control is activated regardless of MAF sensor drift and uncertainty in speed-density equation. Nevertheless, the accuracy of the ethanol estimation is still degraded if an exact MAF drift compensation is not possible due to significant error in the speed density model with degradation of cylinder air flow estimation.

10 CONCLUSION

In this paper, a cylinder air flow estimation scheme under mass air flow sensor drift or bias in order to avoid severe misestimation of ethanol content in flex fuel vehicles is demonstrated. The high sensitivity of ethanol content estimation using an exhaust gas oxygen sensor to MAF sensor error is reviewed. Possible error accumulation problem in correcting MAF sensor drift commonly using an exhaust gas oxygen sensor with ethanol content estimation via a switching scheme is elucidated. To obtain a more reliable cylinder air flow estimation by compensating the MAF sensor drift, the intake manifold pressure sensor signal is utilized together with the speed density principle at selected operating regions. The proposed algorithm inevitably involves switching on correction of MAF sensor drift at operating regions where there is high confidence that the speed density model has high accuracy. However, if a highly accurate reference engine map is available with high confidence, the error accumulation problem can be alleviated in contrast to the switching adaptation case using the λ (EGO) sensor. Simulation is performed to demonstrate the air flow estimation with compensation of MAF sensor drift using an intake manifold pressure sensor and realistic assumption on engine modeling accuracy, and the ethanol content estimation in flex fuel vehicles.

REFERENCES

[1] Theunissen, F., "Percent ethanol estimation on sensorless multi-fuel systems; advantages and limitations". *SAE paper 2003-01-3562*.

[2] Ahn, K., Stefanopoulou, A. G., and Jankovic, M., 2008. "Estimation of ethanol content in flex-fuel vehicles using an exhaust gas oxygen sensor: Model, tuning and sensitivity". In Proceedings of ASME 1st Annual Dynamic Systems and Control Conference.

[3] Delgado, R. C., Araujo, A. S., and Fernandes Jr., V. J., 2007. "Properties of Brazilian gasoline mixed with hydrated ethanol for flex-fuel technology". *Fuel Processing Technology,* **88**(4), pp. 365–368.

[4] Nakata, K., Utsumi, S., Ota, A., Kawatake, K., Kawai, T., and Tsunooka, T., "The effect of ethanol fuel on a spark ignition engine". *SAE paper 2006-01-3380*.

[5] Cowart, J. S., Boruta, W. E., Dalton, J. D., Dona, R. F., Rivard II, F. L., Furby, R. S., Piontkowski, J. A., Seiter, R. E., and Takai, R. M., "Powertrain development of the 1996 Ford flexible fuel Taurus". *SAE paper 952751*.

[6] Stodart, A., Maher, J., Greger, L., and Carlsson, J., "Fuel system development to improve cold start performance of a flexible fuel vehicle". *SAE paper 982532*.

[7] Orbital Engine Co., 2002. "A literature review based assessment on the impacts of a 20% ethanol gasoline fuel blend on the Australian vehicle fleet". *Report to Environment Australia*, Nov.

[8] Bromberg, L., Cohn, D. R., and Heywood, J. B., 2007. "Optimized fuel management system for direct injection ethanol enhancement of gasoline engines". United StatesPatent No. 7225787 B2.

[9] BOSCH, 2000. *Automotive Handbook*, fifth ed.

[10] Batteh, J. J., and Curtis, E. W., "Modeling transient fuel effects with alternative fuels". *SAE paper 2005-01-1127*.

[11] BOSCH. *MAP Sensor Technical Specifications*.

[12] BOSCH. *HFM2-Air Mass Meter*.

[13] Stotsky, A., and Kolmanovsky, I., 2002. "Application of input estimation techniques to charge estimation and control in automotive engines". *Control Engineering Practice,* **10**(12), pp. 1371 – 1383.

[14] Grizzle, J., Cook, J., and Milam, W., 1994. "Improved cylinder air charge estimation for transient air fuel ratio control". *American Control Conference, 1994,* **2**, pp. 1568–1573.

[15] Crossley, P. R., and Cook, J. A., 1991. "A nonlinear engine model for drivetrain system development". *IEE International Conference, Control '91,* **2**, Mar., pp. 921–925.

[16] Ahn, K., Stefanopoulou, A. G., and Jankovic, M., 2009. "Fuel puddle model and AFR compensator for gasoline-ethanol blends in flex-fuel engines". In Proceedings of IEEE Vehicle Power and Propulsion (VPP) Conference.